Accepted Manuscript

A label-free electrochemical biosensor for direct detection of RACK 1□b□y using disposable, low-cost and reproducible ITO based electrode

Hakan Törer, Elif Burcu Aydın, Mustafa Kemal Sezgintürk

PII: S0003-2670(18)30513-0

DOI: 10.1016/j.aca.2018.04.031

Reference: ACA 235891

To appear in: *Analytica Chimica Acta*

Received Date: 15 February 2018

Revised Date: 29 March 2018

Accepted Date: 5 April 2018

Please cite this article as: H. Törer, E.B. Aydın, M.K. Sezgintürk, A label-free electrochemical biosensor for direct detection of RACK 1□b□y using disposable, low-cost and reproducible ITO based electrode, *Analytica Chimica Acta* (2018), doi: 10.1016/j.aca.2018.04.031.

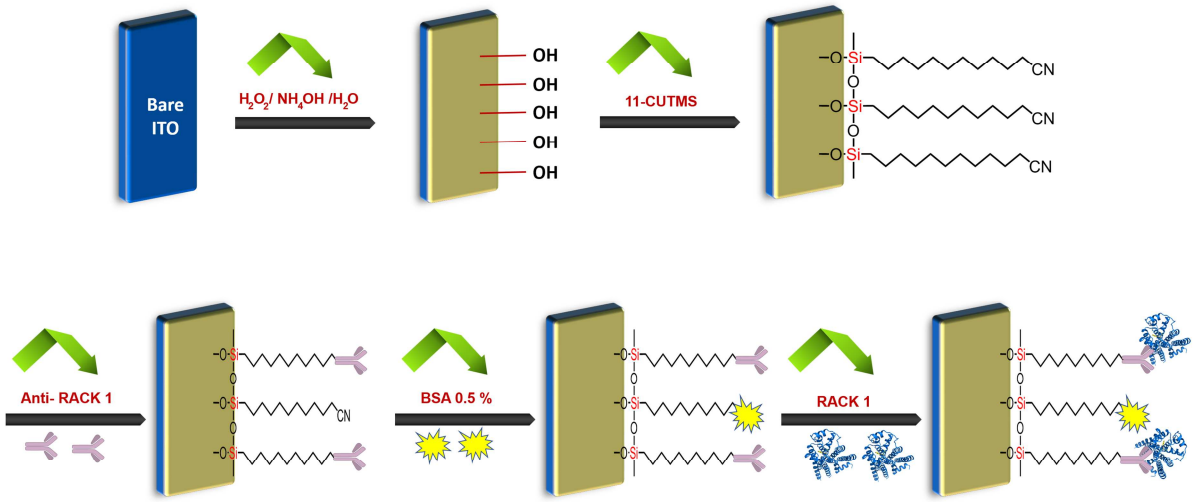

A label-free electrochemical biosensor for direct detection of RACK 1 by using disposable, low-cost and reproducible ITO based electrode

Hakan Törer[a], Elif Burcu Aydın[b], Mustafa Kemal Sezgintürk[c*]

[a]Namık Kemal University, Faculty or Arts and Sciences, Chemistry Department, Tekirdağ-TURKEY

[b]Namık Kemal University, Scientific and Technological Research Center, Tekirdağ-TURKEY

[c]Çanakkale Onsekiz Mart University, Faculty of Engineering, Bioengineering Department, Çanakkale-TURKEY

***Corresponding Author:**

e-mail: msezginturk@hotmail.com

msezginturk@comu.edu.tr

Tel: +90 286 218 00 18

Abstract

In this study we designed an ultrasensitive electrochemical immunosensor for RACK 1 detection using 11-cyanoundecyltrimethoxysilane (11-CUTMS) as a immobilization matrix to immobilize biorecognition element. The used silane agent (11-CUTMS) provides a favorable platform for efficient loading of anti-RACK 1 antibody. The effective loading of the biorecognition element on the 11-CUTMS matrix was monitored by scanning electron microscopy (SEM), atomic force microscopy (AFM) images and fourier transform infrared spectroscopy (FTIR) spectra. The electrochemical characterization of the immunosensor was performed by using electrochemical impedance spectroscopy (EIS) and cyclic voltammetry (CV) techniques. Moreover, biorecognition interaction between anti-RACK1 antibodies and RACK1 antigens was monitored by using single frequency technique (SFI). The operating conditions, calibration curves obtained during optimization of experiments and reproducibility of the proposed impedimetric RACK1 biosensor are also investigated and discussed. The electrochemical immunosensor illustrated a sensitive response to RACK 1 antigen with detection limit of 10.8 fg/mL and in the linear range of 0.036 – 2.278 pg/mL (R^2=0.999). Owing to high specificity, good reproducibility, long stability and reusability, the fabricated immunosensor will provide a sensitive, selective approach to RACK 1 detection. Furthermore, the practical applicability in human serum samples were investigated with a satisfactory result.

Keywords: Receptor of activated C kinase; RACK1; 11-cyanoundecyltrimethoxysilane; ITO; biosensor.

1. Introduction

Receptor of activated C kinase (RACK1) is a 36 kDa cytosolic protein with a propeller-like structure of seven WD40 repeats and belongs to a WD40 superfamily of proteins, including the β subunit of G-proteins. The WD40 repeats of RACK1 play a role in complex protein–protein interactions among signaling molecules such as β integrins, phosphodiesterase 4D5, and Src tyrosine kinase, as well as protein kinase C (PKC) [1-3]. It was first identified as an anchoring protein for protein kinase C (PKC). After RACK1 bound to β-PKC, PKC kinase activity was induced. RACK1 participates in signal transduction, immune defense, cell growth, migration, and differentiation [4-6]. These results suggest that RACK1 might share a function in carcinogenesis, as reported in multiple tumor types, including oral squamous cell carcinoma [1, 7], melanoma, colon cancer [1], non-small cell lung cancer, hepatocellular carcinoma and breast cancer [8, 9].

The ultrasensitive determination of target proteins by using electrochemical immunosensors play a significant role in clinical diagnosis. They have several advantages such as ease of operation, fast analysis, low cost and high sensitivity [10]. In label-free immunosensors, the antibody-antigen complex formation causes a change in thickness of the electrode surface, that blocks electron transfer. In quantitative analysis, determination of target protein is performed by monitoring of changes in electrochemical properties [11].

Tin doped indium oxide (ITO) is a unique transparent conductive material and it has been used in many applications such as photovoltaic cell, optoelectronic devices and biosensors. In biosensor application, ITO is used as a planar electrode due to its good optical transparency, wide working potential, high electrical conductivity, high stability, feasibility and easy miniaturization [12, 13]. In this study, ITO was used as a biosensing platform for electrochemical impedance spectroscopy (EIS) measurements. The effective immobilization of the biorecognition element on ITO surface is important. Therefore, different methods have been used for modification of ITO slices such as physical adsorption [14], electrophoretic deposition [15-17], electrochemical deposition [18, 19], silanization [20, 21], self-assembled monolayer formation [22] and electro-polymerization [23-25]. ITO electrodes were modified with different silane agents such as 3-isocyanatopropyl triethoxysilane (IPTES) [26], 3-aminopropyltriethoxy silane (APTES) [27-29], (3-glycidoxypropyl)trimethoxysilane [30], N-(2-aminoethyl)-3-aminopropyltrimethoxysilane [20], 3-mercaptopropyl trimethoxysilane (3-MPTMS) [31], 3-glycidoxy propyldimethoxysilane [21], 11-(triethoxysilyl)undecanal (TESU) [32] have been utilized in literature and they have caught the attention of many electrochemists due to their unique layer formation and easy formation features. The principle of silanization is based on self-assembled monolayer (SAM) formation on the hydroxylated ITO electrode. SAM layer on the ITO electrode has benefits such as simplicity, stability, reusability, good reproducibility. SAM formation via silane agent provides ITO electrode useful functional ends groups such as -CN, -COOH, $-NH_2$, -SH to bind to biorecognition element. These end groups bind to biomolecules and facilitate electron transfer between biomolecules and electrode surface. The most important benefit of silane reagent usage is the formation of well-controlled layer for immobilization of biomolecules [20, 33].

Electrochemical impedance spectroscopy (EIS) is an effective method to monitor the property of modified electrode surface. This technique has been utilized to investigate the configuration and function of several biosensors such as immunosensors, DNA and enzyme based biosensors [34-36]. Impedimetric immunosensors have attracted interest in recent years due to their direct and label-free measurement ability [37-39]. In this study, apart from EIS technique, for an extensive electrochemical surface characterization of the electrodes single frequency impedance technique was used. Single frequency Impedance (SFI) technique is an informative technique to monitor the interaction between RACK1 antigen and anti-RACK1 antibody. This technique is able to control the biosensor with a total time and a repeat time [40, 41]. Furthermore, FTIR was used to monitor functional groups on modified ITO; SEM and AFM were used for morphological characterization of the fabricated ITO immunosensor.

The goal of this study is the fabrication of a new, stable, sensitive and regenerative ITO based immunosensor for detection of RACK1 biomarker. ITO electrode surface was firstly modified with 11-cyanoundecyltrimethoxysilane (CUTMS) then with anti-RACK1 antibody and finally with BSA. 11-CUTMS was utilized as a self-assembled layer material and it constructed a bridge between ITO electrode and the biorecognition element (anti-RACK1). The electrochemical behaviors of the immunosensor were analyzed by cyclic voltammetry (CV) and EIS. The optimum operating conditions, calibration curves obtained during optimization of experiments and reproducibility of impedimetric RACK1 biosensor are also investigated and discussed. This developed immunosensor had a wide linear detection range (0.036-2.278 pg/mL) and low LOD (10.8 fg/mL). The results obtained from real human serum samples showed that ITO based immunosensor had encouraging perspectives in the field of electroanalysis. Another significant point was successive regeneration of the developed immunosensor. Although disposable electrode was used, it could be regenerated. This feature of the electrode provides lower analysis cost. The impedimetric results indicate that RACK1 antigen can be easily and sensitively detected by the new immunosensor. Furthermore, the obtained results showed that the developed immunosensor can be utilized to determine RACK 1 in human serum samples successfully.

2. Experimental details

2.1 Reagents

All chemicals were of analytical grade and utilized directly for the experiments without further purification and the aqueous solutions were prepared with ultra-pure water. ITO coated Polyethylene Terephthalate (PET) films (resistance of 60 Ω/square; thickness of ITO layer 150 nm), 11-cyanoundecyltrimethoxysilane (CUTMS), anti-RACK1 antibody, RACK1 antigen and BSA were obtained from Sigma-Aldrich. Anti-RACK1 antibody, RACK1 antigen and BSA (0.5%) were prepared with phosphate buffer (50 mM pH 7.0) and were stored at -20 ^{o}C until they were used. Ferri-ferro solution, a redox probe, was prepared by using 5 mM $K_4[Fe(CN)_6]/K_3[Fe(CN)_6]$.

2.2 Apparatus

The EIS, CV, SFI studies were carried out on a Gamry Potentiostat/Galvonstat (Reference 1000, Gamry Instruments, Warminster, PA, USA). A three-electrode system was utilized in our study. The CUTMS modified ITO electrode (2*20 mm), Ag/AgCl electrode, platinium electrode were utilized as working electrode (WE), reference electrode (RE), and counter electrode (CE), respectively. The RE, CE were purchased from BASi (West Lafayette, IN, USA). The surface topography of modified ITO electrode surface was monitored with SEM measurements using a FEI-Quanta FEG 250 Model microscope at an operating voltage 5 kV. AFM images were attained using a NanoMagnetics Instruments-AFM Plus Model. All AFM images were recorded in tapping mode with a commercial tapping silicon tip and the estimated tip radius was less than 10 nm. To monitor surface end groups, FTIR (Bruker Vertex 70 ATR Model) was utilized. The measurements were performed at the range of 4000-400 cm^{-1} and the results were used without any corrections. The SEM, AFM and FTIR measurements were carried out at the Scientific and Technological Research Center of NKU (NABILTEM).

2.3 Procedures

2.3.1 Preparation of Working Electrode

ITO coated PET-films were cleaned in ultrasonic bath by using solutions of acetone, soap solution and ultra-pure water for at least 10 min each. Then, they were treated in a solution of $H_2O_2/NH_4OH/H_2O$ (1:1:5) for 90 min at room temperature to attain hydroxylated active ITO surface. Finally, they were rinsed with ultra-pure water and were dried under argon gas.

2.3.2 Fabrication of CUTMS-modified RACK1 immunosensor

The activated ITO thin films were immersed 0.5% CUTMS solution prepared in toluene overnight. The ITO/CUTMS thin films were then rinsed with toluene and ultra-pure water to remove non-bonded 11-CUTMS silane molecules from PET film surface and dried under argon gas. After that CUTMS modified ITO thin films immersed into PBS solution containing anti-RACK1 antibodies. For immobilization of anti-RACK1 antibodies, the amount of antibody used was optimized. The ITO/CUTMS/anti-RACK1 electrode washed thoroughly with ultra-pure water. At the last step of fabrication, BSA (0.5%) was used to block free silane ends of modified ITO. The fabrication process of impedimetric immunosensor was illustrated in scheme 1. At the end of these steps our immunosensor was ready for RACK1 detection.

2.3.3 Electrochemical Measurements

All electrochemical experiments were performed with a potentiostat/galvanostat and the electrochemical features of the modified ITO electrodes were monitored by using CV and EIS. The operation parameters for CV measurements are as follows; scan rate: 100 mVs^{-1} and step size 10 mV, for EIS measurement; initial

frequency: 50000 Hz, final frequency: 0.05 Hz, points:5, for SFI measurements; frequency: 20 Hz, repeat time 0.01 min, total time 0.5 h.

3. Results and Discussion

3.1 Design Procedure of the impedimetric RACK1 Immunosensor

Fabrication of RACK1 immunosensor consists of four stages: (i) cleaning and hydroxylation of ITO slices, (ii) silanization of hydroxylated ITO electrode (iii) immobilization of anti-RACK1 antibody onto the CUTMS modified ITO electrode via amidine bond between the nitrile group of CUTMS and amino group of antibody (iv) blocking of free CUTMS ends to prevent nonspecific interaction. Biosensing procedure and electrochemical detection of RACK1 are shown in Scheme 1.

Scheme 1. Schematic representation of biosensing procedure and electrochemical detection of RACK1 antigen

The modification process of the immunosensor was observed by EIS and CV. EIS is an effective technique for characterization of the interface features of electrodes. [$Fe(CN)^{3-/4-}$] was utilized a redox active probe to monitor electrochemical behavior of ITO electrode [42]. Figure 1A displays the Nyquist diagrams of each electrode involving different construction steps of the impedimetric biosensor. Nyquist plots of the electrodes include a semi-circle and linear portion. The semicircle at higher frequencies and a linear part at lower frequencies is related to electron transfer and diffusion processes, respectively. The diameter of semicircle part shows the electron transfer resistance (R_{ct}). A change in the value of R_{ct} is related to the blocking effect of the stepwise modification procedure of the impedimetric immunosensor. The impedance values are fitted to standard Randle's equivalent circuit, that includes the ohmic resistance of the electrolyte solution (R_s), surface double-layer capacitance (CdI), Warburg impedance (Z_w) that is originated from the diffusion of ions from the bulk of the electrolyte to the electrode interface, and charge transfer resistance (R_{ct}) (Figure 1A inset). Ideally, Z_w and R_s show the features of the electrolyte solution and diffusion of the redox probe, so they are not affected from modifications that occurred on the electrode surface. In addition, Cdl and R_{ct} are associated to the dielectric and insulating properties at the electrode/electrolyte interface, therefore they are affected by the variations occurred on the electrode surfaces [43, 44].

Figure 1. Impedance spectra (A) and cyclic voltammograms (B) of the RACK 1 immunosensor during the fabrication steps; Randles equivalent circuit (inset)

When CUTMS layer successively immobilized on the ITO surface, the R_{ct} value increased due to SAMs insulator property. In addition, a repulsive interaction was occurred between the negative charged CUTMS and anionic redox probe occurred and the diameter of Nyquist plot was increased. Thus, negatively charged redox probe could not be diffused easily to the electrode surface. After immobilization of anti-RACK 1 antibodies on the ITO/CUTMS electrode, a semicircle with fairly large diameter was monitored. This

illustrated that immobilized antibodies increase the impedance. Observed increase in the value of R_{ct} was attributed to the electron transfer hindrance of the antibody macromolecules. In the next step, BSA immobilized on the non-binding sites on the ITO electrode and BSA hindered the electron transfer between the medium and electrode so the R_{ct} value was increased. The Nyquist plot illustrated the expected increase in R_{ct} after incubation with RACK 1 antigen; as seen Figure 1A indicated that a specific interaction was formed.

Furthermore, the fabrication steps of the biosensing surface were examined by CV measurements. CV analyses of hydroxylated and modified electrodes were carried out to characterize electrochemical changes occurred on the ITO electrode surface and redox features of biosensor. Figure 1B displays the cyclic voltammograms of each step of electrode surface modification. Modified ITO electrode surface showed a quite reversible cyclic voltammogram. As it is seen in figure 1B, hydroxylated ITO electrode had high anodic-cathodic peak currents. After modification of hydroxylated ITO with CUTMS self-assembled layer, the redox peak currents were decreased. SAM formation hindered the diffusion of the ferri-ferro ions toward negatively charged surface of CUTMS SAMs. In the case of anti-RACK 1 protein immobilization, a decrease was obtained due to the interaction between nitrile groups on the electrode surface and amino groups of antibody. In the BSA immobilization step, it blocked non-specific binding sites (active nitrile groups) of ITO electrode. After the addition of BSA, the peak current decreased remarkably, which indicated that a lot of non-specific binding sites were blocked by BSA. As can be seen from pink line (after BSA) and blue line (after interaction between anti-RACK 1 and RACK 1 antigen), a decrease in the pink current was monitored after introducing RACK 1 on the electrode surface. Consequently, it can be considered that a specific interaction was formed successfully. After all immobilization steps, the immunosensor was ready for the determination of RACK 1 antigen.

3.2 FTIR Studies

In this study, the FTIR spectrometer was used for investigation of chemical reaction between nitrile group of immobilization matrix on modified ITO electrode and amino groups of anti-RACK1 antibodies. The FTIR spectra of CUTMS modified ITO electrode and antibody immobilized ITO electrode are shown in Figure 1. The FTIR spectrum of CUTMS modified ITO electrode (Figure 1a) presented the characteristic absorption peak at 2243 cm^{-1} (–C≡N), which indicated that the self-assembly layer were formed completely [45]. The FTIR spectra confirmed that the amino group was introduced onto the CUTMS modified ITO surface (figure 1b). The peak at 1650 cm^{-1} in the FTIR spectrum of modified ITO electrode ratified that amino groups in anti-RACK 1 antibodies were covered on the electrode surface [46].

Figure 2. FTIR spectra of CUTMS modified ITO electrode (A) and after anti-RACK 1 immobilization on the ITO electrode (B)

3.3 Morphological characterization of the modified electrodes

Fig. 3 shows micrographs of the biosensor surfaces obtained by SEM and AFM along different steps of the immunosensor construction. The SEM and AFM images revealed that a uniform CUTMS layer were formed on ITO substrate in Figure 3A and Figure 3B, respectively. The root mean square (RMS) roughness was found as 5 nm on a 5×5 µm scale. The thickness of CUTMS layer should be thicker than the height expected for a monolayer. In addition, the results presented that the proposed immunosensor had good analytical performance and the formed mono- or multilayer did not affect the performance of the proposed immunosensor. The changes on the ITO electrode surface after anti-RACK 1 antibody immobilization are illustrated in Figure 3C and Figure 3D. It can be clearly seen that the antibodies were bound on the surface and an uneven surface was formed. After antibody immobilization step, the roughness value of 25.85 nm on a 5×5 µm scale was achieved. After blockage of nitrile groups by BSA, the surface structure of the electrode was changed as seen in Figure 3E and Figure 3F. The RMS roughness value of 31.18 nm on 5×5 µm scale was found after BSA blockage step. Figure 3G and Figure 3H illustrate the SEM and AFM images after anti-RACK 1 antibody and RACK 1 antigen interactions. As seen in SEM image (Figure 3G), RACK1 antigen presented a flower-like morphology which is in good agreement with AFM observations and the RMS value was found as 26.95 nm on 5×5 µm scale.

Figure 3. SEM and AFM images of CUTMS modified ITO electrode (A, B), after anti-RACK 1 immobilization (C, D), BSA blockage (E and F), after specific interaction between anti-RACK 1 antibody and RACK 1 antigen (G and H).

3.4 Optimization of Experimental Parameters

A lot of experiments were performed to select optimum analytical conditions. To obtain a sensitive, stable biosensor with effective catalytic features, optimization experiments of immobilization steps had a great importance. These experiments were CUTMS concentration optimization, anti-RACK 1 binding period and concentration optimization, RACK 1 binding period optimization. All of the experiment were performed at room temperature. Each optimization step was characterized by using electrochemical methods such as EIS, CV.

In the first step of the study, CUTMS concentration used for SAM formation was optimized. This step was important for binding of adequate amount of biorecognition molecules, anti-RACK 1 antibodies, on the electrode surface. Therefore, three different concentrations (0.1%; 0.5%; 1% w/w) were tried. CUTMS had two groups; silane groups on the one end and nitrile on the other. These silane ends bound to ITO electrode surface after hydroxylation processes of ITO electrode. The usage of 0.1% concentration of CUTMS was inadequate to form SAM on the ITO electrode. The using of 1% concentration of 11-CUTMS caused deterioration and for this reason, regular signals were not obtained. The best signals were obtained after using 0.5% concentration of CUTMS. According to the obtained data, a standard curve was drawn by using

R_{ct} values in the EIS. The obtained signals and also standard curves are shown in figure SI-1. Anti-RACK 1 antibody concentration was the second optimization parameter. This step was important because the amount of linked biorecognition element affect the sensitivity, stability and detection range of the developed biosensor. To choose optimum anti-RACK 1 concentration, three different concentrations was utilized; 0.4062 pg/mL; 0.8125 pg/mL and 1.625 pg/mL. The highest change in R_{ct} values was obtained by using anti-RACK 1 antibody with 0.4062 pg/mL concentration. Therefore, 0.4062 pg/mL anti-RACK 1 concentration was chosen optimum antibody concentration. The obtained calibration curves after usage of these concentrations are shown in figure SI-2. To find the optimum RACK 1 antibody incubation period, CUTMS modified ITO electrodes incubated in anti-RACK 1 solution for 45 and 60 min. The highest signal was obtained after 45 min incubation period. Therefore, 45 min was chosen as the optimum incubation period for antibody binding. The low antibody concentration (0.4062 pg/mL) and short incubation period (45 min) decreases the fabrication cost of the biosensor and provides time-saving. The calibration curves belonging to each period are shown in figure SI-3. Finally, the influence of the immunoreaction time, in other words incubation period of RACK 1 antigen was studied. As seen figure SI-4, the change in R_{ct} were nearly same after 30 min, 45 min, 60 min incubation period. The maximum signal was observed at 30 min. Thus, 30 min was used for subsequent experiments and short incubation period provides time-saving.

3.5 Analytical performance (features) of the immunosensor

Before investigation of the analytical performance of the biosensor, the effect of four parameters such as CUTMS concentration, anti-RACK 1 antibody concentration and incubation time and RACK 1 antigen incubation time on the performance of the proposed immunosensor were studied. The biosensor analytical performance experiments were carried out by determination of different RACK 1 concentration under optimized conditions. Change in R_{ct} values was investigated and calculated by the following equation:

$\Delta R_{ct}=R_{ct}(\text{RACK 1})- R_{ct}(\text{BSA})$

Where R_{ct}(RACK 1) is the value of R_{ct} when RACK 1 antigen incubated with immobilized antibody, R_{ct}(BSA) is the R_{ct} of immunosensor after BSA blockage.

Figure 4. Impedance spectra and cyclic voltammograms of the immunosensor after incubation with different concentrations of RACK 1 antigen (A and B), Calibration curve of RACK 1 (C), SFI spectra of after specific interaction between RACK 1 antibody and RACK 1 antigen (D).

A relationship was found between the impedance changes and the concentration of RACK 1 antigen and the linear detection range was between 0.035 pg/mL and 2.2784 pg/mL. This linear detection graph of the proposed immunosensor is illustrated in figure 4C. The linear regression equation was ΔR_{ct}= 2557 [RACK 1]-17.554 (R^2=0.999). Limit of detection (LOD) for the immunosensor was determined to be 10.8 fg/mL which was obtained based on the signal of blank sample/slope ratio of three. Limit of Quantification (LOQ)

for the immunosensor was determined to be 36 fg/mL, that was obtained based on the signal of blank sample/slope of ten.

Figure 4 illustrates impedance spectra, CV voltammograms and the calibration curve of the developed immunosensor. As seen in figure 4A and 4B, there were an increase in diameter of Nyquist plots and a decrease in peak currents, respectively. When these results were considered, it was concluded that a linear increase in the R_{ct} value and a linear decrease in the peak current value of fabricated immunosensor were a function of analyte concentration. The cause of this increase and this decrease were the formation of additional kinetic barrier by RACK 1 antigens, thus the entrance of the redox couple to the electrode surface was limited.

Single frequency impedance analysis is a method that illustrates the specific interaction between antibody-antigen, probe DNA-target DNA. The basic principle of this technique is based on the measurement of the impedance at a fixed frequency versus time. Firstly, the frequency that will be used in studies are determined by using Bode Plot. The usage reason of Bode Plot is providing the impedance data as a function of frequency. In this study, optimum frequency value was chosen as 20 Hz. Blue curve and red curve (in figure 4D) illustrates the change in the impedance and the change in the phage angle as a function of time, respectively. A significant change in impedance confirmed the interaction between RACK 1 antibody and RACK 1 antigen. These obtained results showed that single frequency impedance can be utilized for sensing and biosensing monitoring, for evaluation of slow time-dependent changes on a sensor surface [40, 46].

Repeatability, reproducibility are two important properties for practical utilization of the immunosensors. Repeatability analyses were investigated using different 20 electrodes. The low relative standard deviation (RSD 4.52%) of repeatability analysis indicated that the developed impedimetric biosensor had good repeatability. The reproducibility of the fabricated impedimetric immunosensor was investigated by constructing 7 biosensors (with equally prepared 49 electrodes) to detect RACK 1. The calibration plots of these biosensors are shown Figure SI-5. Reproducibility is a vital parameter in the performance of the prepared impedimetric immunosensor. The low RSD (4.89%) for the impedimetric biosensor has an acceptable reproducibility.

Regeneration is an important parameter in reducing the cost of the biosensor. In regeneration analysis, biosensor was prepared as mentioned above. Firstly, ITO electrode with anti-RACK 1 antibody on its surface incubated in PBS solution containing RACK 1 antigen. Then, it was incubated in a HCl solution (10 mM, 5 min). The aim of this regeneration was break down the specific interaction that occurred between antibody and antigen Following this, the regenerated surface was incubated with RACK 1 solution (0.57 pg/mL) again. During both of these two experiments, biosensor signals were measured. Consequently, our biosensor was regenerated 4 times. In the 5^{th} regeneration step, the surface of the biosensor was damaged and it lost 30% of its initial activity (Figure SI-6).

Stability of a biosensor is a key parameter in sensor development and application. The stability of ITO/CUTMS/anti-RACK 1/BSA electrode was evaluated by measuring impedance of constant RACK 1 concentration over a period of 10 weeks. The signal of the biosensor retains approximately 88.8% after 8 weeks, when it was stored at 4 ^{o}C in dry form. These results confirmed that the new immunosensor had satisfactory stability (The storage stability results are shown in Figure SI-7).

Selectivity is also significant during practical utilization of a immunosensor. The feasibility of the immunosensor for clinical applications was analyzed using real samples of human serum. To test selectivity of the proposed biosensor, different interferences such as biomarkers (Sex-determining region Y-box 2 (SOX2), Melanoma associated antigen 1 (MAGE 1), Tumor necrosis factor a (TNF α)) and drugs (ampicillin, ciprofloxacin, erythromycin) were added PBS solution containing RACK 1 antigen and without RACK 1 antigen. As seen Fig. SI-8, these interferences did not affect the biosensor signal. RACK 1 levels in human serum was found at nanogram level by Bahadır and Sezgintürk (2016), which is outside of the linear range of this impedimetric biosensor. For this reason, the human serum was diluted 1:100000 in PBS to reduce RACK 1 levels to a desired concentration. Results obtained from serum and after subsequent addition of RACK 1 are displayed in Table 1. The acceptable recoveries ranging from 91.0% to 109.2% were obtained also the result showed that the biosensor is suitable for potential practical applications.

Table 1. The results of serum samples obtained by the proposed immunosensor

4. Conclusion

In this study, we described a novel RACK 1 biosensor fabricated by immobilizing anti-RACK 1 antibody by silanization method on the disposable low-cost ITO electrode. For the modification of biosensor, CUTMS with nitrile ends was used and it formed a self-assembled layer on ITO surface. This sensing platform exhibited good loading surface of anti-RACK 1 antibodies. After optimization of experimental conditions, a sensitive and cheap biosensor was produced. This immunosensor had a wide linear range (0.035-2.2784 pg/mL), acceptable reproducibility (RSD 4.52%), good repeatability (RSD 4.89%) and long stability (88.8% signal after 8 weeks). Furthermore, this biosensor was disposable, but after regeneration it could be used for 4 times. This feature decreases the production cost of the biosensor. The applicability of biosensor in human serum was confirmed by standard addition method. Moreover, in this study we analyzed the fabrication steps of immunosensor by using SEM and AFM for morphological characterization. All of these results confirmed the successful fabrication of the immunosensor.

Acknowledgment

The financial support from TÜBİTAK (The Scientific and Technological Research Council of Turkey, Project number: 113 Z 678) is gratefully acknowledged.

5. References

[1] R. Nagashio, Y. Sato, T. Matsumoto, T. Kageyama, Y. Satoh, R. Shinichiro, N. Masuda, N. Goshima, S.-X. Jiang, I. Okayasu, Expression of RACK1 is a novel biomarker in pulmonary adenocarcinomas, Lung cancer, 69 (2010) 54-59.
[2] D.R. Adams, D. Ron, P.A. Kiely, RACK1, A multifaceted scaffolding protein: Structure and function, Cell communication and signaling, 9 (2011) 22.
[3] S. Kraus, D. Gioeli, T. Vomastek, V. Gordon, M.J. Weber, Receptor for activated C kinase 1 (RACK1) and Src regulate the tyrosine phosphorylation and function of the androgen receptor, Cancer research, 66 (2006) 11047-11054.
[4] Q. Ren, J. Zhou, X.-F. Zhao, J.-X. Wang, Molecular cloning and characterization of a receptor for activated protein kinase C1 (RACK1) from Chinese white shrimp; Fenneropenaeus chinensis, Developmental & Comparative Immunology, 35 (2011) 629-634.
[5] Z. Wang, B. Zhang, L. Jiang, X. Zeng, Y. Chen, X. Feng, Y. Guo, Q. Chen, RACK1, an excellent predictor for poor clinical outcome in oral squamous carcinoma, similar to Ki67, European Journal of Cancer, 45 (2009) 490-496.
[6] Y. Ikebuchi, K. Ito, T. Takada, N. Anzai, Y. Kanai, H. Suzuki, Receptor for activated C-kinase 1 regulates the cell surface expression and function of ATP binding cassette G2, Drug Metabolism and Disposition, 38 (2010) 2320-2328.
[7] T.B. Schaaij-Visser, R.H. Brakenhoff, C.R. Leemans, A.J. Heck, M. Slijper, Protein biomarker discovery for head and neck cancer, Journal of proteomics, 73 (2010) 1790-1803.
[8] X.X. Cao, J.D. Xu, X.L. Liu, J.W. Xu, W.J. Wang, Q.Q. Li, Q. Chen, Z.D. Xu, X.P. Liu, RACK1: A superior independent predictor for poor clinical outcome in breast cancer, International journal of cancer, 127 (2010) 1172-1179.
[9] X.-X. Cao, J.-D. Xu, J.-W. Xu, X.-L. Liu, Y.-Y. Cheng, W.-J. Wang, Q.-Q. Li, Q. Chen, Z.-D. Xu, X.-P. Liu, RACK1 promotes breast carcinoma proliferation and invasion/metastasis in vitro and in vivo, Breast cancer research and treatment, 123 (2010) 375-386.
[10] Y. Liu, L.-P. Xu, S. Wang, W. Yang, Y. Wen, X. Zhang, An ultrasensitive electrochemical immunosensor for apolipoprotein E4 based on fractal nanostructures and enzyme amplification, Biosensors and Bioelectronics, 71 (2015) 396-400.
[11] H. Haji-Hashemi, P. Norouzi, M.R. Safarnejad, M.R. Ganjali, Label-free electrochemical immunosensor for direct detection of Citrus tristeza virus using modified gold electrode, Sensors and Actuators B: Chemical, 244 (2017) 211-216.
[12] X.R. Cheng, B.Y. Hau, T. Endo, K. Kerman, Au nanoparticle-modified DNA sensor based on simultaneous electrochemical impedance spectroscopy and localized surface plasmon resonance, Biosensors and Bioelectronics, 53 (2014) 513-518.
[13] E.B. Aydın, M.K. Sezgintürk, Indium Tin Oxide (ITO): A promising material in biosensing technology, TrAC Trends in Analytical Chemistry, (2017).
[14] C.M. Pandey, S. Dewan, S. Chawla, B.K. Yadav, G. Sumana, B.D. Malhotra, Controlled deposition of functionalized silica coated zinc oxide nano-assemblies at the air/water interface for blood cancer detection, Analytica chimica acta, 937 (2016) 29-38.
[15] S. Kumar, S. Kumar, S. Tiwari, S. Augustine, S. Srivastava, B.K. Yadav, B.D. Malhotra, Highly sensitive protein functionalized nanostructured hafnium oxide based biosensing platform for non-invasive oral cancer detection, Sensors and Actuators B: Chemical, 235 (2016) 1-10.
[16] I. Tiwari, M. Singh, C.M. Pandey, G. Sumana, Electrochemical genosensor based on graphene oxide modified iron oxide–chitosan hybrid nanocomposite for pathogen detection, Sensors and Actuators B: Chemical, 206 (2015) 276-283.
[17] A. Sharma, D. Baral, H. Bohidar, P.R. Solanki, Oxalic acid capped iron oxide nanorods as a sensing platform, Chemico-biological interactions, 238 (2015) 129-137.
[18] A. Singh, M. Choudhary, M. Singh, H. Verma, S.P. Singh, K. Arora, DNA functionalized direct electro-deposited gold nanoaggregates for efficient detection of Salmonella typhi, Bioelectrochemistry, 105 (2015) 7-15.
[19] A.K. Yagati, J.-C. Pyun, J. Min, S. Cho, Label-free and direct detection of C-reactive protein using reduced graphene oxide-nanoparticle hybrid impedimetric sensor, Bioelectrochemistry, 107 (2016) 37-44.

[20] L. Yang, Y. Li, AFM and impedance spectroscopy characterization of the immobilization of antibodies on indium–tin oxide electrode through self-assembled monolayer of epoxysilane and their capture of Escherichia coli O157: H7, Biosensors and Bioelectronics, 20 (2005) 1407-1416.
[21] M.B. dos Santos, S. Azevedo, J. Agusil, B. Prieto-Simon, C. Sporer, E. Torrents, A. Juárez, V. Teixeira, J. Samitier, Label-free ITO-based immunosensor for the detection of very low concentrations of pathogenic bacteria, Bioelectrochemistry, 101 (2015) 146-152.
[22] E.B. Aydın, M. Aydın, M.K. Sezgintürk, A highly sensitive immunosensor based on ITO thin films covered by a new semi-conductive conjugated polymer for the determination of TNFα in human saliva and serum samples, Biosensors and Bioelectronics, (2017).
[23] S. Komathi, A.I. Gopalan, K.-P. Lee, Fabrication of a novel layer-by-layer film based glucose biosensor with compact arrangement of multi-components and glucose oxidase, Biosensors and Bioelectronics, 24 (2009) 3131-3134.
[24] W. Chu, Q. Zhou, S. Li, W. Zhao, N. Li, J. Zheng, Oxidation and sensing of ascorbic acid and dopamine on self-assembled gold nanoparticles incorporated within polyaniline film, Applied Surface Science, 353 (2015) 425-432.
[25] N. Prabhakar, Z. Matharu, B. Malhotra, Polyaniline Langmuir–Blodgett film based aptasensor for ochratoxin A detection, Biosensors and Bioelectronics, 26 (2011) 4006-4011.
[26] M. Ozmen, K. Can, M. Ersoz, Immobilization of albumin on indium-tin oxide (ITO) surface via isocyanate linkage, Journal of Electroanalytical Chemistry, 633 (2009) 228-234.
[27] M.Ç. Canbaz, M.K. Sezgintürk, Fabrication of a highly sensitive disposable immunosensor based on indium tin oxide substrates for cancer biomarker detection, Analytical biochemistry, 446 (2014) 9-18.
[28] G.-I. Kim, K.-W. Kim, M.-K. Oh, Y.-M. Sung, Electrochemical detection of vascular endothelial growth factors (VEGFs) using VEGF antibody fragments modified Au NPs/ITO electrode, Biosensors and Bioelectronics, 25 (2010) 1717-1722.
[29] Y. Wang, W. Qian, Y. Tan, S. Ding, H. Zhang, Direct electrochemistry and electroanalysis of hemoglobin adsorbed in self-assembled films of gold nanoshells, Talanta, 72 (2007) 1134-1140.
[30] D. Guo, M. Zhuo, X. Zhang, C. Xu, J. Jiang, F. Gao, Q. Wan, Q. Li, T. Wang, Indium-tin-oxide thin film transistor biosensors for label-free detection of avian influenza virus H5N1, Analytica chimica acta, 773 (2013) 83-88.
[31] A.K. Yagati, T. Lee, J. Min, J.-W. Choi, Electrochemical performance of gold nanoparticle–cytochrome c hybrid interface for H 2 O 2 detection, Colloids and Surfaces B: Biointerfaces, 92 (2012) 161-167.
[32] E.B. Bahadır, M.K. Sezgintürk, Label-free, ITO-based immunosensor for the detection of a cancer biomarker: Receptor for Activated C Kinase 1, Analyst, 141 (2016) 5618-5626.
[33] S.K. Arya, A.K. Prusty, S. Singh, P.R. Solanki, M.K. Pandey, M. Datta, B.D. Malhotra, Cholesterol biosensor based on N-(2-aminoethyl)-3-aminopropyl-trimethoxysilane self-assembled monolayer, Analytical biochemistry, 363 (2007) 210-218.
[34] J. Filip, S. Zavahir, L. Klukova, J. Tkac, P. Kasak, Immobilization of concanavalin A lectin on a reduced graphene oxide-thionine surface by glutaraldehyde crosslinking for the construction of an impedimetric biosensor, Journal of Electroanalytical Chemistry, 794 (2017) 156-163.
[35] X.Y. Zhang, L.Y. Zhou, H.Q. Luo, N.B. Li, A sensitive and label-free impedimetric biosensor based on an adjunct probe, Analytica chimica acta, 776 (2013) 11-16.
[36] A.A. Moya, A Numerical Exercise To Teach Electrochemical Impedance Using Electric Circuit Simulation Software, ACS Publications, 2013.
[37] M. Hoyos-Nogués, S. Brosel-Oliu, N. Abramova, F.-X. Muñoz, A. Bratov, C. Mas-Moruno, F.-J. Gil, Impedimetric antimicrobial peptide-based sensor for the early detection of periodontopathogenic bacteria, Biosensors and Bioelectronics, 86 (2016) 377-385.
[38] E. Sheikhzadeh, M. CHamsaz, A. Turner, E. Jager, V. Beni, Label-free impedimetric biosensor for Salmonella Typhimurium detection based on poly [pyrrole-co-3-carboxyl-pyrrole] copolymer supported aptamer, Biosensors and Bioelectronics, 80 (2016) 194-200.
[39] A. Bogomolova, E. Komarova, K. Reber, T. Gerasimov, O. Yavuz, S. Bhatt, M. Aldissi, Challenges of electrochemical impedance spectroscopy in protein biosensing, Analytical chemistry, 81 (2009) 3944-3949.
[40] B. Özcan, B. Demirbakan, G. Yeşiller, M.K. Sezgintürk, Introducing a new method for evaluation of the interaction between an antigen and an antibody: Single frequency impedance analysis for biosensing systems, Talanta, 125 (2014) 7-13.
[41] L. Hou, Y. Ding, L. Zhang, Y. Guo, M. Li, Z. Chen, X. Wu, An ultrasensitive competitive immunosensor for impedimetric detection of microcystin-LR via antibody-conjugated enzymatic biocatalytic precipitation, Sensors and Actuators B: Chemical, 233 (2016) 63-70.

[42] S. Wang, Y. Zhang, J. Yu, X. Song, S. Ge, M. Yan, Application of indium tin oxide device in gold-coated magnetic iron solid support enhanced electrochemiluminescent immunosensor for determination of carcinoma embryonic antigen, Sensors and Actuators B: Chemical, 171 (2012) 891-898.
[43] L. Alfonta, A. Bardea, O. Khersonsky, E. Katz, I. Willner, Chronopotentiometry and Faradaic impedance spectroscopy as signal transduction methods for the biocatalytic precipitation of an insoluble product on electrode supports: routes for enzyme sensors, immunosensors and DNA sensors, Biosensors and Bioelectronics, 16 (2001) 675-687.
[44] Y. Huang, M.C. Bell, I.I. Suni, Impedance biosensor for peanut protein Ara h 1, Analytical chemistry, 80 (2008) 9157-9161.
[45] F. Huang, Y. Xu, S. Liao, D. Yang, Y.-L. Hsieh, Q. Wei, Preparation of amidoxime polyacrylocyanide chelating nanofibers and their application for adsorption of metal ions, Materials, 6 (2013) 969-980.
[46] E.B. Aydın, M.K. Sezgintürk, A sensitive and disposable electrochemical immunosensor for detection of SOX2, a biomarker of cancer, Talanta, 172 (2017) 162-170.

Figures, Scheme and Table Legends

Scheme 1. Schematic illustration of the fabrication protocol of proposed immunosensor

Table 1. RACK 1 determination by using the proposed immunosensor in human serum

Figure 2. FTIR spectra before and after anti-RACK 1 immobilization

Figure 1. Impedance measurements (A), cyclic voltammograms (B) and the equivalent circuit model used for fitting of the impedance data (inset)

Figure 3. SEM and AFM images of biosensor construction steps

Figure 4. Nyquist plots (A) and cyclic voltammograms (B) for different concentrations of RACK 1, calibration curve of RACK-1 biosensor (C), Single Frequency Impedance result (D)

Table 1.

Sample	Found by biosensor (pg/mL)	Added RACK 1 (pg/mL)	Total found by biosensor	% Recovery	% Relative Difference
1	0.05	0.57	0.58	93.55	6.45
2	0.06	0.57	0.598	94.92	5.08
3	0.065	0.57	0.64	100.79	-0.79
4	0.058	0.57	0.604	96.18	3.82
5	0.054	0.57	0.592	94.87	5.13
6	0.057	0.57	0.624	99.52	0.48
7	0.065	0.57	0.627	98.74	1.26
8	0.06	0.57	0.604	95.87	4.13
9	0.054	0.57	0.615	98.56	1.44
10	0.054	0.57	0.606	97.12	2.88

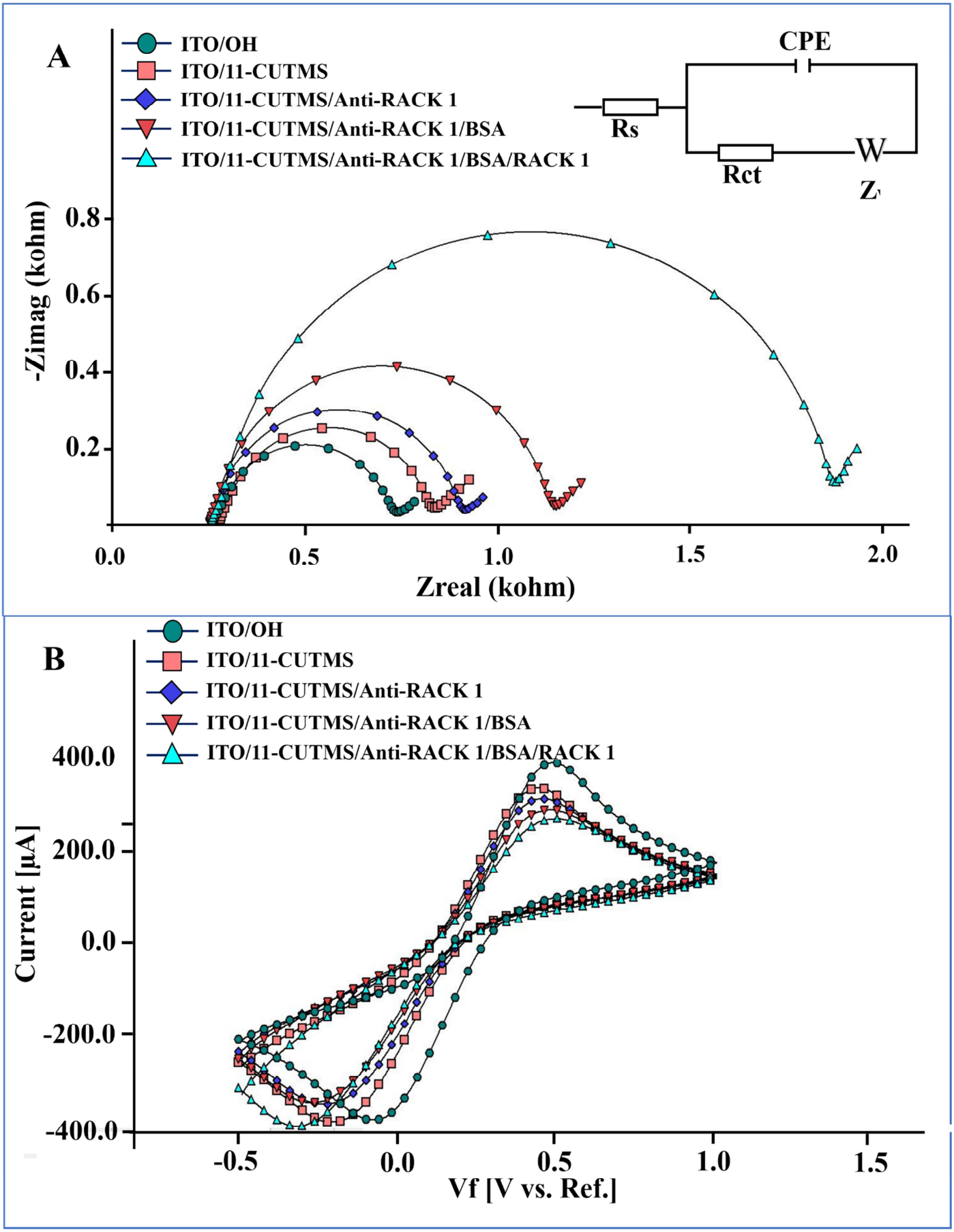
A
ITO/OH
ITO/11-CUTMS
ITO/11-CUTMS/Anti-RACK 1
ITO/11-CUTMS/Anti-RACK 1/BSA
ITO/11-CUTMS/Anti-RACK 1/BSA/RACK 1
CPE
Rs
Rct
W
Z
-Zimag (kohm)
0.8
0.6
0.4
0.2
0.0
0.5
1.0
1.5
2.0
Zreal (kohm)
B
ITO/OH
ITO/11-CUTMS
ITO/11-CUTMS/Anti-RACK 1
ITO/11-CUTMS/Anti-RACK 1/BSA
ITO/11-CUTMS/Anti-RACK 1/BSA/RACK 1
400.0
200.0
0.0
-200.0
-400.0
Current [µA]
-0.5
0.0
0.5
1.0
1.5
Vf [V vs. Ref.]

Figure 1

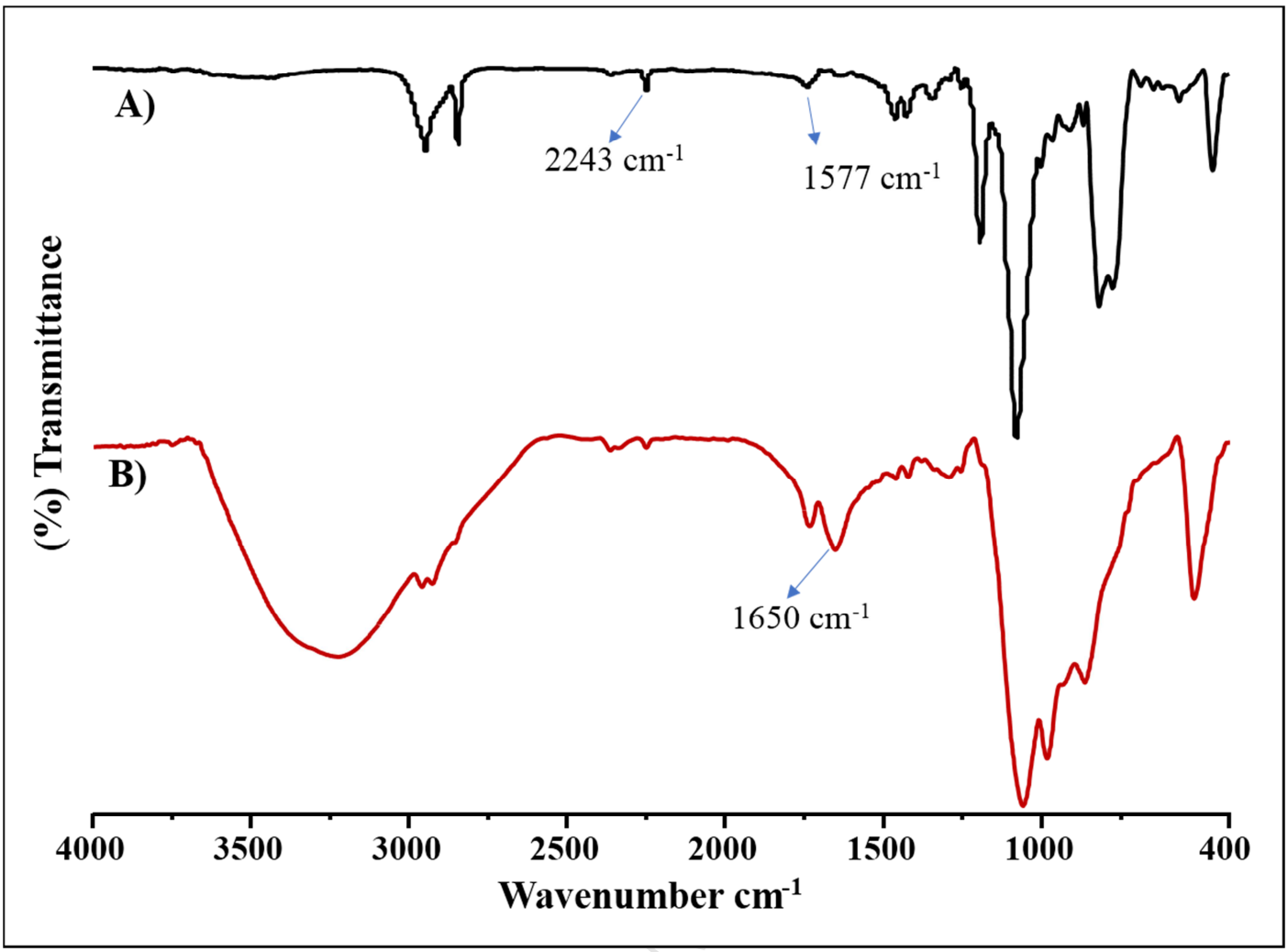

Figure 2

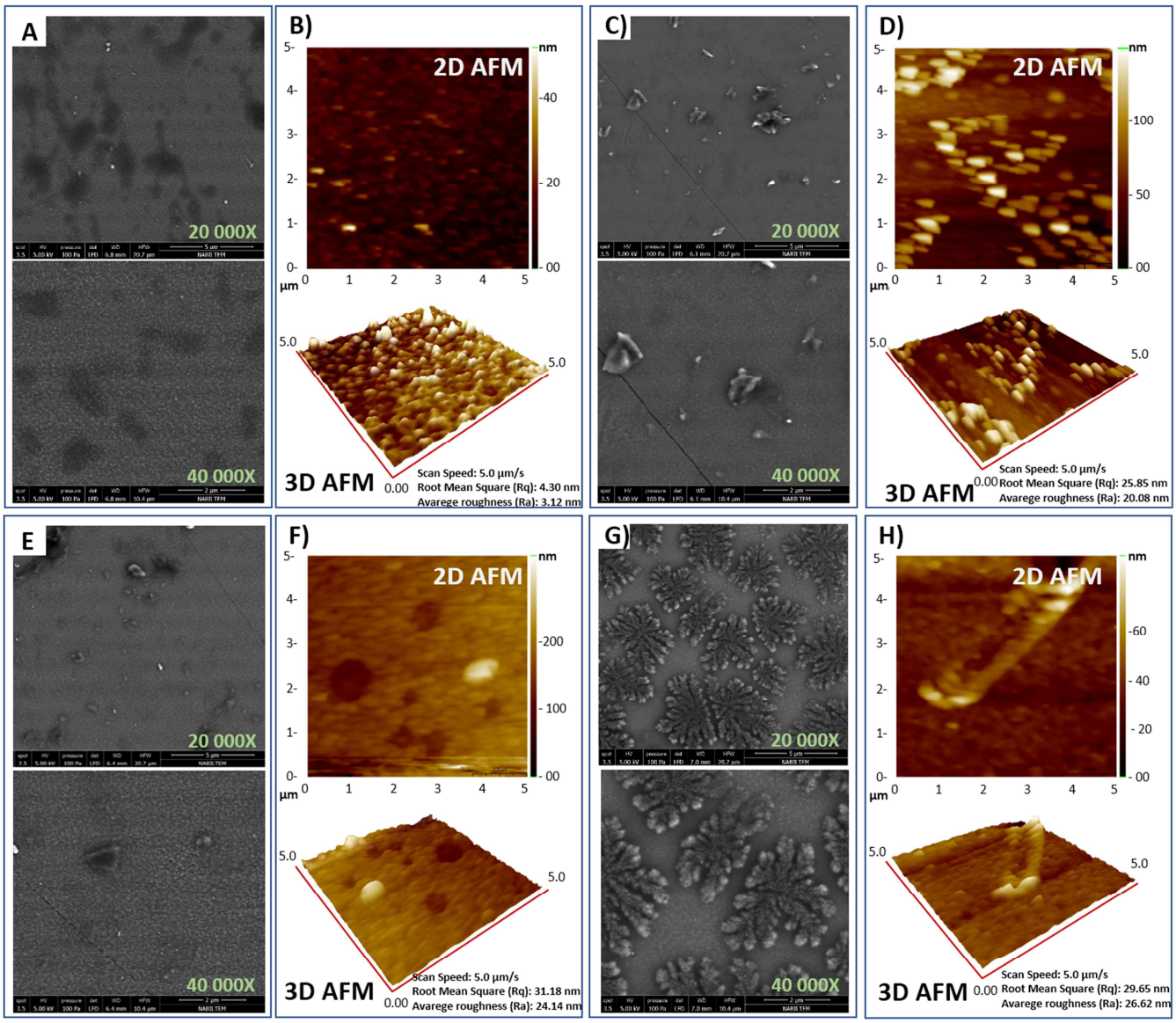
A
20 000X
40 000X
B)
2D AFM
nm
-40
-20
-00
µm
3D AFM
Scan Speed: 5.0 µm/s
Root Mean Square (Rq): 4.30 nm
Avarege roughness (Ra): 3.12 nm
C)
20 000X
40 000X
D)
2D AFM
-100
-50
3D AFM
Scan Speed: 5.0 µm/s
Root Mean Square (Rq): 25.85 nm
Avarege roughness (Ra): 20.08 nm
E
20 000X
40 000X
F)
2D AFM
-200
-100
3D AFM
Scan Speed: 5.0 µm/s
Root Mean Square (Rq): 31.18 nm
Avarege roughness (Ra): 24.14 nm
G)
20 000X
40 000X
H)
2D AFM
-60
-40
-20
3D AFM
Scan Speed: 5.0 µm/s
Root Mean Square (Rq): 29.65 nm
Avarege roughness (Ra): 26.62 nm

BSA

Figure 3

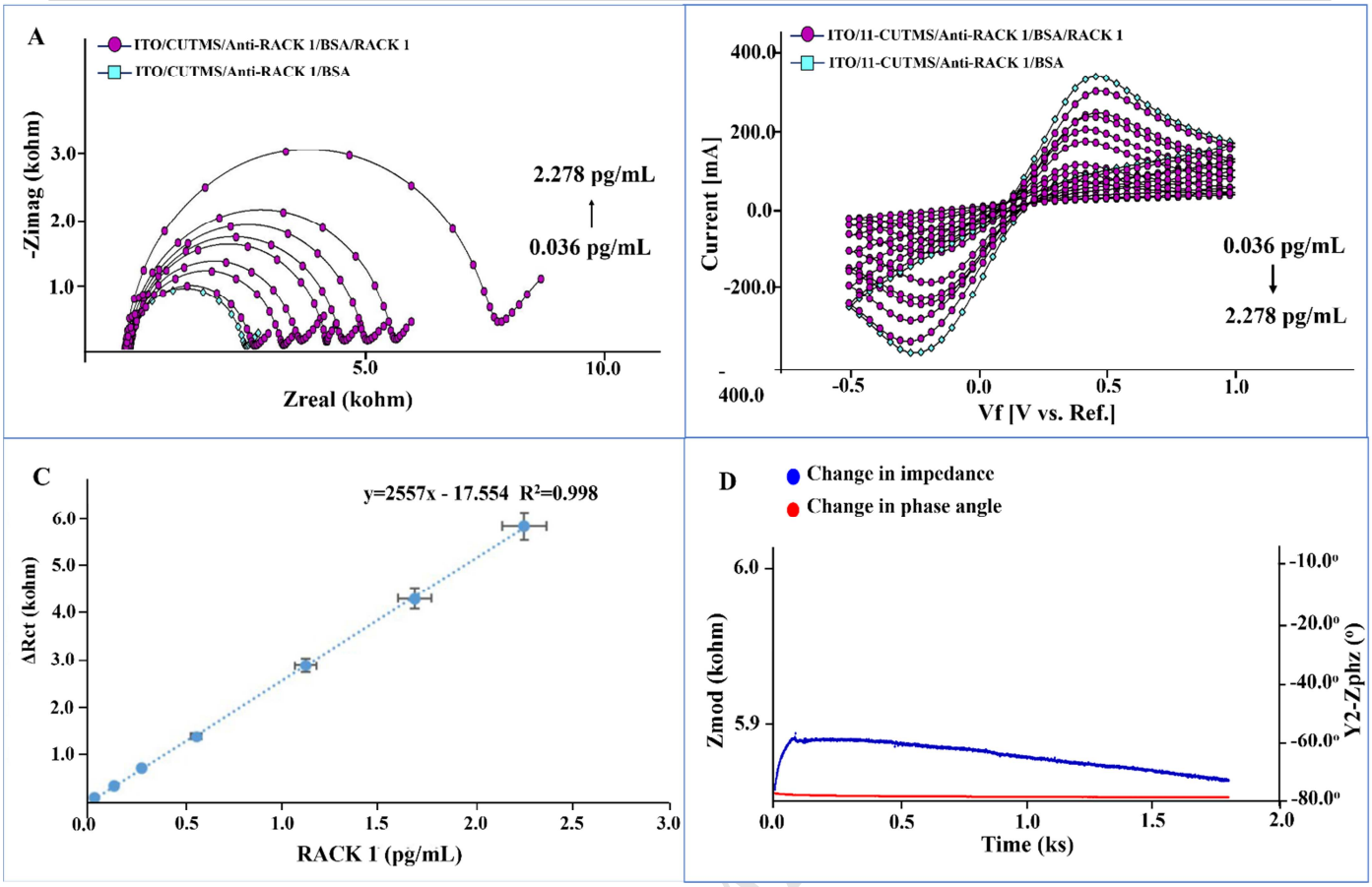

Figure 4

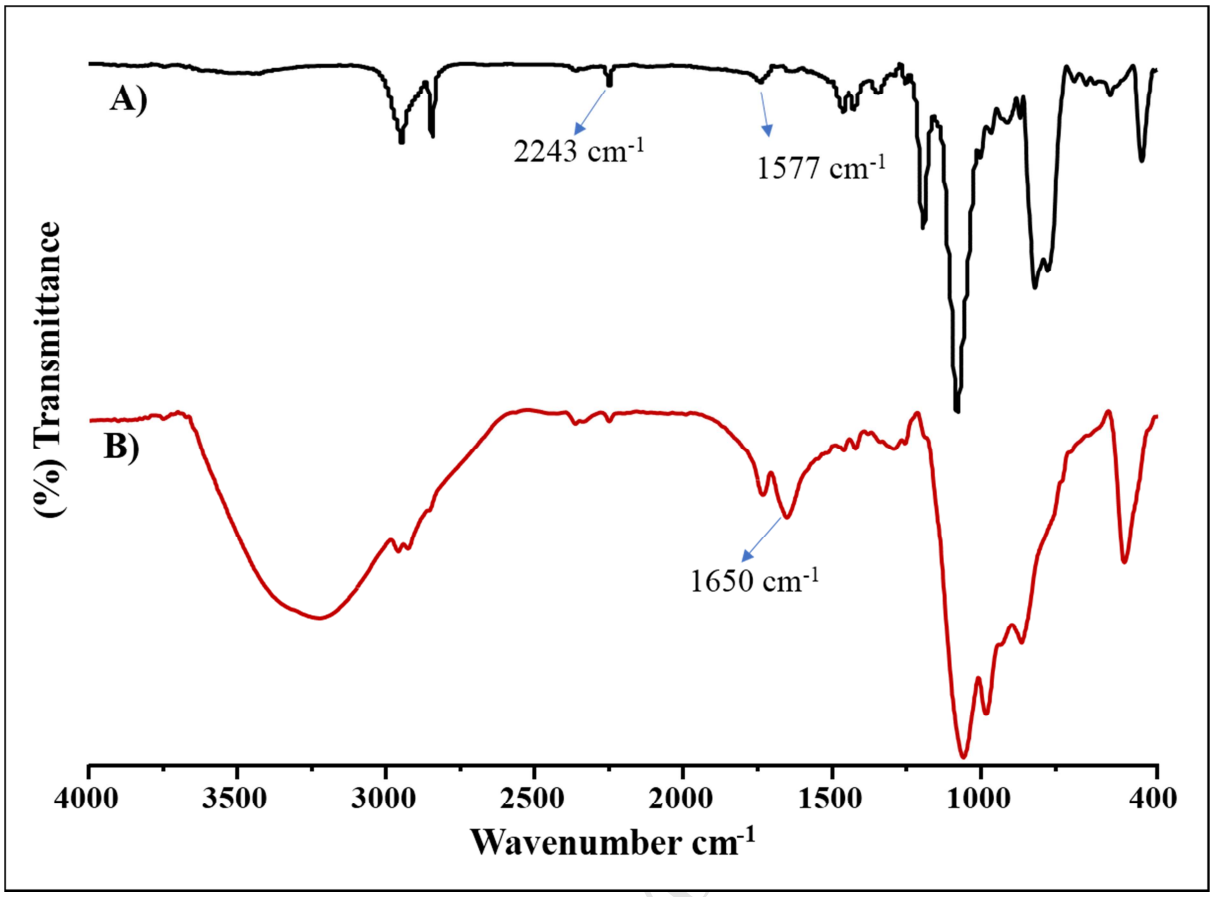

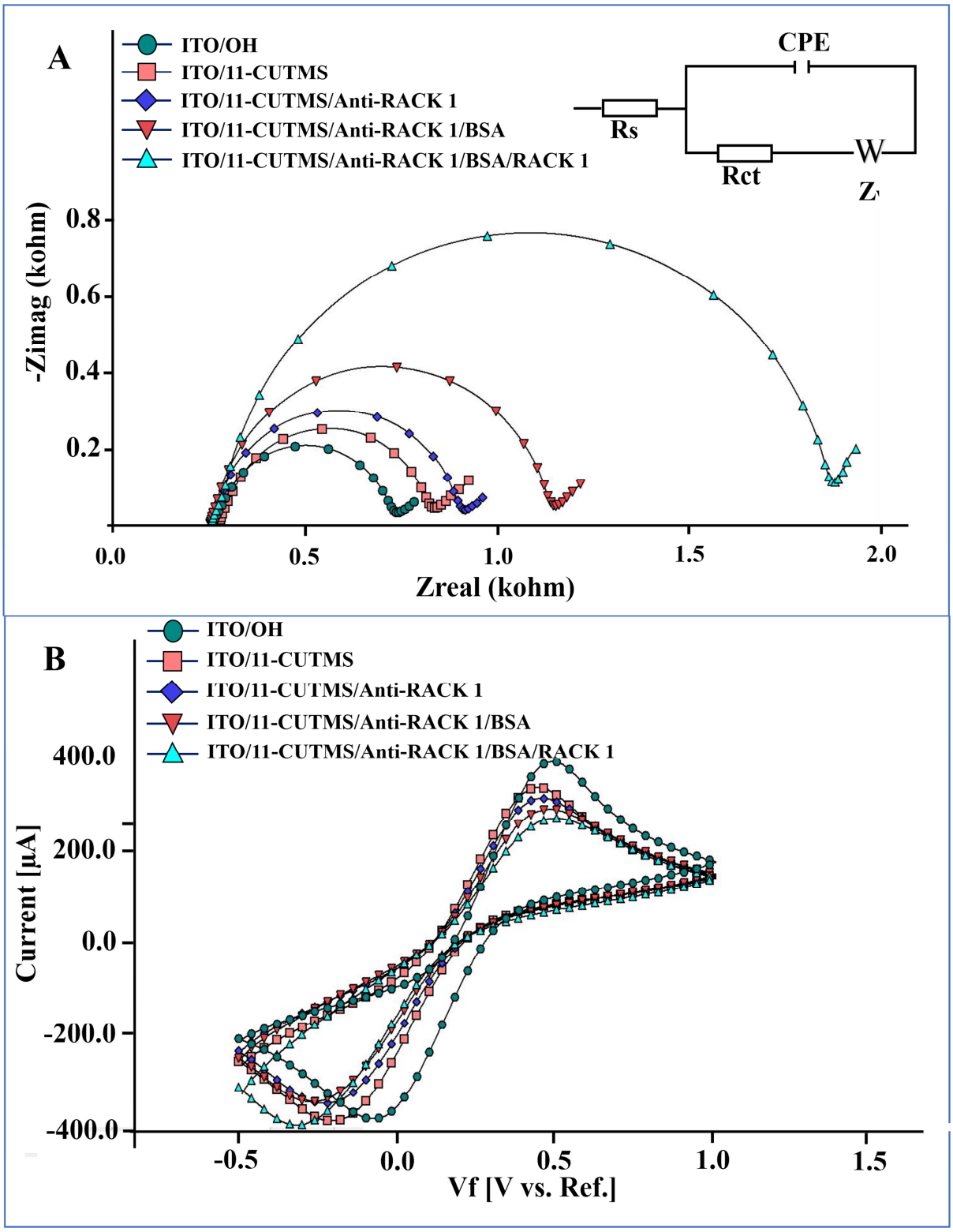
A
ITO/OH
ITO/11-CUTMS
ITO/11-CUTMS/Anti-RACK 1
ITO/11-CUTMS/Anti-RACK 1/BSA
ITO/11-CUTMS/Anti-RACK 1/BSA/RACK 1
CPE
Rs
Rct
W
-Zimag (kohm)
0.8
0.6
0.4
0.2
0.0
0.5
1.0
1.5
2.0
Zreal (kohm)
B
ITO/OH
ITO/11-CUTMS
ITO/11-CUTMS/Anti-RACK 1
ITO/11-CUTMS/Anti-RACK 1/BSA
ITO/11-CUTMS/Anti-RACK 1/BSA/RACK 1
400.0
200.0
0.0
-200.0
-400.0
Current [µA]
-0.5
0.0
0.5
1.0
1.5
Vf [V vs. Ref.]

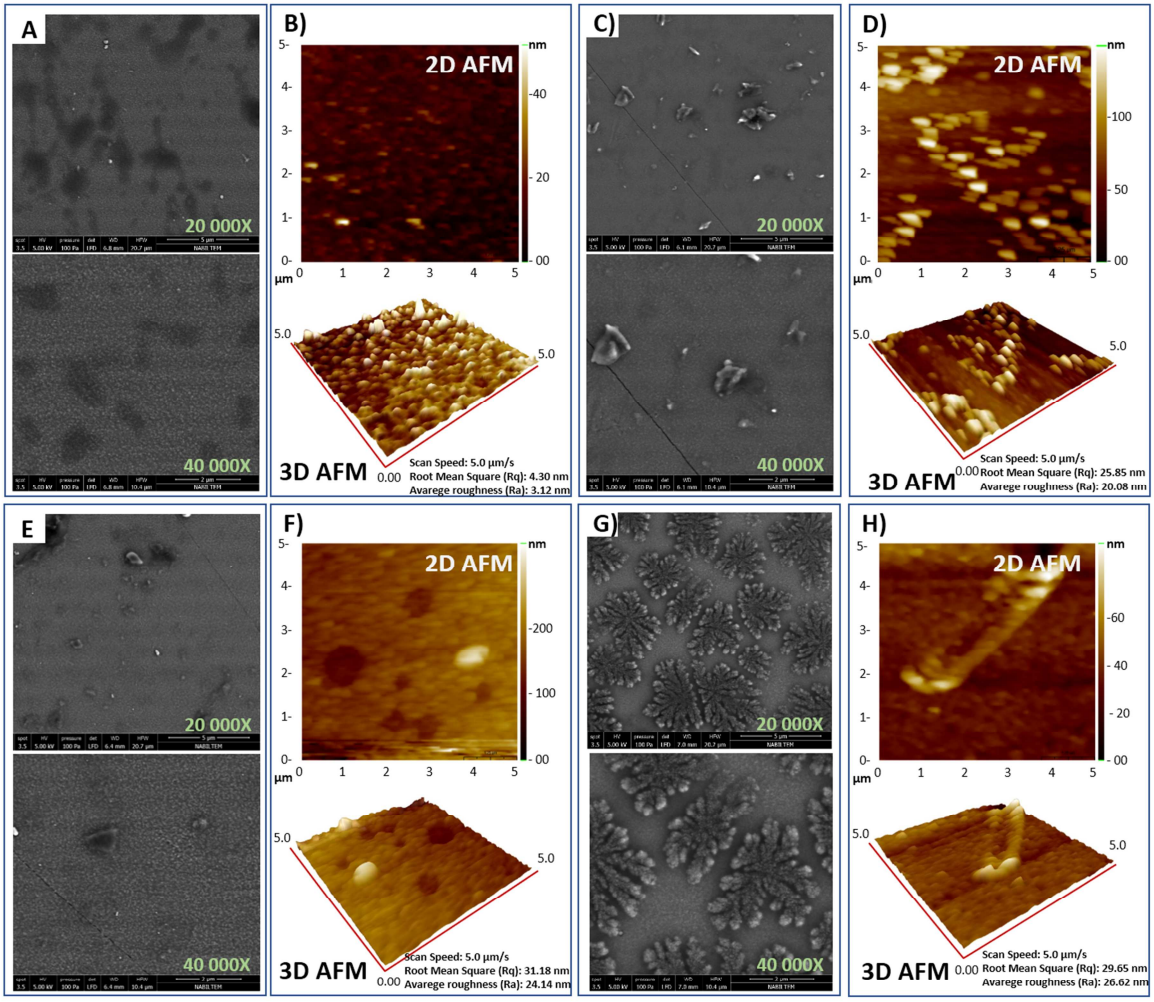

BSA

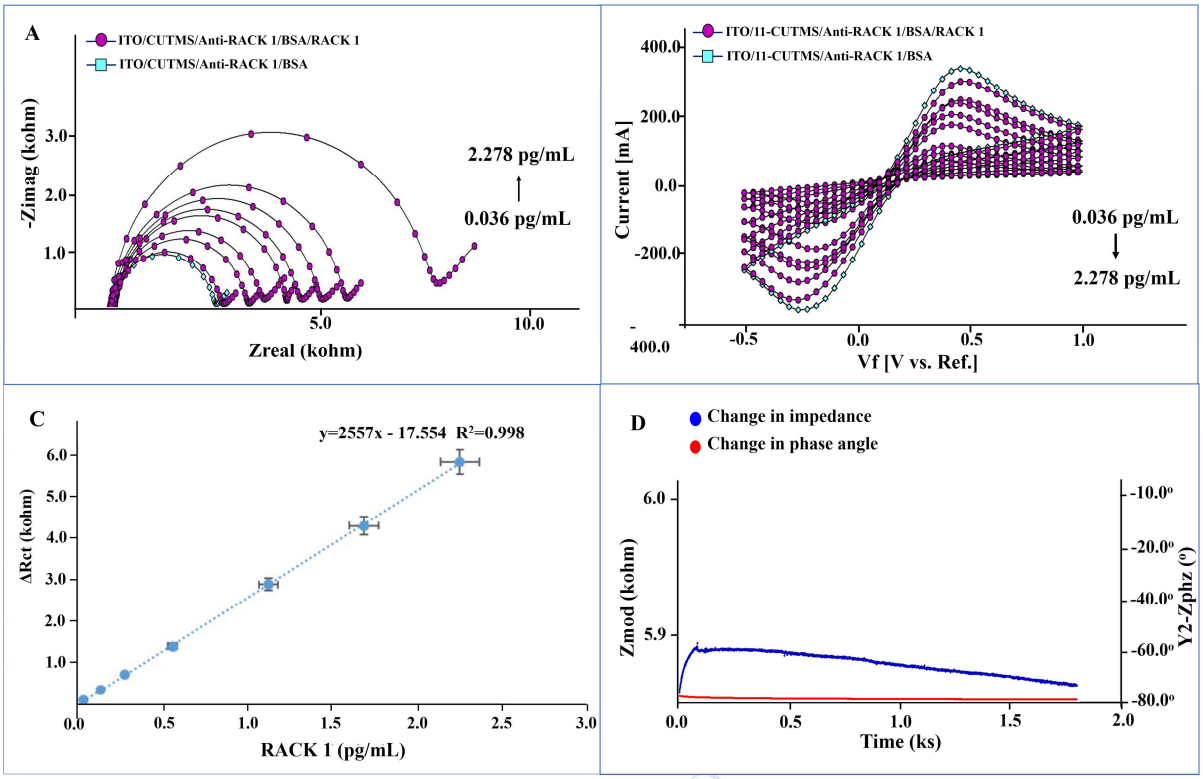

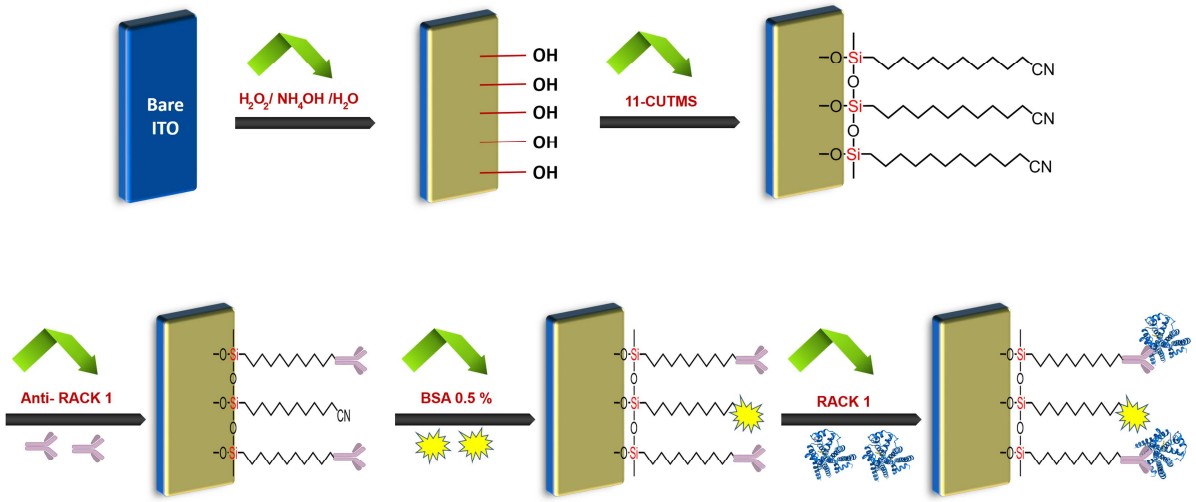

The Highlights:

An highly sensitive, disposable, ITO based biosensor was developed for the analysis of RACK-1.

Anti-RACK-1 antibody as a biorecognition component was immobilized on ITO substrate.

CV, EIS, SEM, AFM, and FT-IR methods were used for characterization of the electrode surfaces.

The new biosensor presents highly analytical performance with a linear range 0.036 – 2.278 pg/mL with a LOD value of 10.8 fg/mL RACK-1.